Received: 1 March 2019 | Revised: 9 May 2019 | Accepted: 3 June 2019

DOI: 10.1111/anec.12679

ORIGINAL ARTICLE

WILEY

Classification of drug-induced hERG potassium-channel block from electrocardiographic T-wave features using artificial neural networks

Micaela Morettini PhD | **Chiara Peroni MS** | **Agnese Sbrollini PhD** | **Ilaria Marcantoni** | **Laura Burattini PhD**

Department of Information Engineering, Università Politecnica delle Marche, Ancona, Italy

Correspondence
Laura Burattini, PhD, Department of Information Engineering, Università Politecnica delle Marche, Via Brecce Bianche, 60131 Ancona, Italy.
Email: l.burattini@univpm.it

Abstract

Background: Human ether-à-go-go-related gene (hERG) potassium-channel block represents a harmful side effect of drug therapy that may cause torsade de pointes (TdP). Analysis of ventricular repolarization through electrocardiographic T-wave features represents a noninvasive way to accurately evaluate the TdP risk in drug-safety studies. This study proposes an artificial neural network (ANN) for noninvasive electrocardiography-based classification of the hERG potassium-channel block.

Methods: The data were taken from the "ECG Effects of Ranolazine, Dofetilide, Verapamil, and Quinidine in Healthy Subjects" Physionet database; they consisted of median vector magnitude (VM) beats of 22 healthy subjects receiving a single 500 μg dose of dofetilide. Fourteen VM beats were considered for each subject, relative to time-points ranging from 0.5 hr before to 14.0 hr after dofetilide administration. For each VM, changes in two indexes accounting for the early and the late phases of repolarization, $\Delta ERD_{30\%}$ and $\Delta T_{S/A}$, respectively, were computed as difference between values at each postdose time-point and the predose time-point. Thus, the dataset contained 286 $\Delta ERD_{30\%}$-$\Delta T_{S/A}$ pairs, partitioned into training, validation, and test sets (114, 29, and 143 pairs, respectively) and used as inputs of a two-layer feed-forward ANN with two target classes: high block (HB) and low block (LB). Optimal ANN (OANN) was identified using the training and validation sets and tested on the test set.

Results: Test set area under the receiver operating characteristic was 0.91; sensitivity, specificity, accuracy, and precision were 0.93, 0.83, 0.92, and 0.96, respectively.

Conclusion: OANN represents a reliable tool for noninvasive assessment of the hERG potassium-channel block.

KEYWORDS

artificial neural network, cardiac repolarization, dofetilide, drug-induced long QT syndrome, hERG channels

1 | INTRODUCTION

Block of the human ether-à-go-go-related gene (hERG) potassium channel represents a harmful side effect of drug therapy (Roden, 2016). The hERG potassium channel carries the rapid component of the delayed rectifier potassium current I_{Kr} (outward current), thus playing a key role in cardiac ventricular repolarization (Mitcheson, Chen, Lin, Culberson, & Sanguinetti, 2000). Block of the hERG potassium channel leads to lower potassium current going outside the cardiac cell, longer cardiac myocyte action potential duration, longer ventricular repolarization, and consequently longer QT interval on the electrocardiogram (ECG). This phenomenon, known as drug-induced long QT syndrome (diLQTS), could predispose to development of torsade de pointes (TdP), a polymorphic ventricular tachycardia. For this reason, investigation of the QT-interval prolongation was used as main hurdle factor for evaluation of the existing drugs and development of new ones (Mitcheson et al., 2000).

Drugs, such as antiarrhythmics, used to treat cardiovascular diseases, but also some antibiotics, anticancer agents, antipsychotics, and antihistamines, are known to prolong the QT interval (Roden, 2016). However, among drugs that block the hERG potassium channels and prolong the QT interval, some have minimal TdP risk. This is attributed to the fact that such drugs cause a multichannel block condition, since they block calcium and late sodium channels, beside potassium channel (Johannesen, Vicente, Gray, et al., 2014). Block of potassium outward current causes an increase in calcium or sodium current, leading to early afterdepolarizations, which constitutes a trigger for TdP. Thus, concomitant blockage of calcium and late sodium current can avoid early afterdepolarizations, thus resulting in a lower TdP risk. Therefore, an investigation based solely on the QT interval is not exhaustive to establish TdP risk attributed to a drug. A deeper analysis of ventricular repolarization through T-wave features can more accurately evaluate TdP risk in drug-safety studies (Johannesen, Vicente, Mason, et al., 2014). Recently, an index combining T-wave down slope and T-wave amplitude has been proposed as an alternate ECG-based metric for quantifying the hERG potassium-channel block, independently from concomitant calcium and/or sodium channels block (De Bie, Chiu, Mortara, Corsi, & Severi, 2017). However, evidence showed that the main ECG difference between a pure hERG blocker and a multichannel blocker drug is that the former prolongs both the early and the late phases of repolarization, whereas the latter preferentially shortens early phase of repolarization (Johannesen, Vicente, Mason, et al., 2014). Thus, features describing both the early and the late phases of repolarization should be combined to provide a comprehensive description of drug effect in terms of TdP risk.

The aim of this study was to propose an artificial neural network (ANN) for classification of the hERG potassium-channel block, having as inputs ECG-based T-wave features on both right and left T-wave sides (with reference to the T-wave peak) to account for the early and the late phases of repolarization. To this aim, ECG acquisitions at various time-points before and after administration of dofetilide, a pure hERG blocker with the highest risk of TdP, quantified in 1÷5% of exposed subjects (Abraham et al., 2015) were considered.

2 | METHODS

2.1 | Study population and clinical data

The data analyzed in this study are available at the "ECG Effects of Ranolazine, Dofetilide, Verapamil, and Quinidine in Healthy Subjects" Physionet database (Goldberger et al., 2000; Johannesen, Vicente, Mason, et al., 2014). The study population consisted of 22 healthy subjects; the inclusion criteria (Johannesen, Vicente, Mason, et al., 2014) required subjects to be of general good health as determined by a physician, without a history of heart disease or unexplained syncope or a family history of long QT syndrome; to be 18–35 years of age, weigh at least 50 kg, and have a body mass index of 18–27 kg/m^2; and to be able to read and understand the informed consent. In addition, subjects were excluded if they had more than 10 ectopic beats during a continuous 3-hr ECG recording at screening. Each subject received a single 500 μg dose of dofetilide under fasting conditions while undergoing continuous 12-lead ECG acquisition (sampling frequency: 500 Hz; amplitude resolution: 2.5 μV). Triplicate 10-s ECG segments were extracted from the continuous recording, at fourteen predefined time-points: one predose time-point (−0.5 hr) and thirteen postdose time-points (1.0; 1.5; 2.0; 2.5; 3.0; 3.5; 4.0; 5.0; 6.0; 7.0; 8.0; 12.0; 14.0 hr). Additionally, at the same 14 time-points, a blood sample was drawn for measuring dofetilide plasma concentration. Triplicate ECG segments and plasma data are available in the Physionet database. All data from Physionet have been fully de-identified and may be used without further independent ethics committee approval.

2.2 | Feature extraction from the ECG signal

Each 10-s 12-lead ECG segment was transformed into a 10-s 3-Frank-orthogonal lead ECG segment from which the median beat of the vector magnitude (VM) lead was derived (these data are available in the Physionet database). Each median VM beat was considered representative of the 10-s ECG segment itself and was used for feature extraction. Hence, a total of 924 median VM beats were analyzed (22 subjects by 14 time-points by three ECG recordings).

From each median VM beat, two T-wave features were selected to account for both the early and the late phases of repolarization, namely $ERD_{30\%}$ (ms) and $T_{S/A}$ (per s). Specifically, $ERD_{30\%}$ represents the 30% early phase of repolarization duration (Vicente et al., 2015) and $T_{S/A}$ is defined as the ratio of down-going T-wave slope (T_{RS}, mV/s) and T-wave amplitude ($T_{A,}$ mV), where T_{RS} is defined as the absolute value (being a downslope) of the mean first derivative of the T wave in the T_pT_e interval (i.e., time interval between T-wave peak and T-wave end). $ERD_{30\%}$, T_A, and T_pT_e for each median VM beat were directly taken from the Physionet database, whereas T_{RS} and $T_{S/A}$ were computed according to their definitions.

In each subject, $ERD_{30\%}$ and $T_{S/A}$ values associated with each of the 14 time-points were computed as the mean value of the three measures obtained from triplicate ECG acquisitions. Successively, $\Delta ERD_{30\%}$ and $\Delta T_{S/A}$ were computed as the difference between the corresponding feature values at each of the thirteen postdose time-point (1.0–14.0 hr) and the predose control time-point (−0.5 hr). Thus, a total of 286 $\Delta ERD_{30\%}$ and $\Delta T_{S/A}$ values were considered.

2.3 | Assessment of the hERG potassium-channel block from plasma measurements

From dofetilide plasma concentration (*D*) measured at each of the thirteen postdose time-points, the percentage of hERG potassium-channel block was estimated from the Hill equation (1):

$$B(\%) = 100 \cdot \frac{D^n}{IC_{50}^n + D^n} \quad (1)$$

where IC_{50} is the drug concentration causing 50% block, and *n* is the Hill coefficient. IC_{50} and *n* values were assumed equal to 1 nM and 0.6, respectively, as reported in literature (Crumb, Vicente, Johannesen, & Strauss, 2016). *B*(%) values were used to classify channel blocks into two classes: high block (HB), when *B*(%) > 60%, and low block (LB), when *B*(%) ≤ 60%. Eventually, plasma-based hERG potassium-channel block classification in HB and LB was used as reference to train, validate, and test the proposed ANN (see below).

2.4 | Artificial neural network for assessing the hERG potassium-channel block

VM features $\Delta T_{S/A}$ and $\Delta ERD_{30\%}$ were used as inputs of a two-layer feedforward ANN (one hidden layer and one output layer) with two output neurons, one for each output target class (HB and LB). As for the activation function, a sigmoid and a softmax function were used in the hidden and in the output layers, respectively (Bishop, 2006). Iterative backpropagation training was ensured by the Levenberg–Marquardt algorithm (Hagan & Menhaj, 1994).

The dataset constituted by the 286 $\Delta ERD_{30\%}$ and $\Delta T_{S/A}$ input pairs and the corresponding 286 plasma-based HB\LB output targets was partitioned into training set, validation set, and test set according to the following percentages: 40% (114 input pairs and HB\LB output targets), 10% (29 input pairs and output targets), and 50% (143 input pairs and output targets), respectively. Overall, 20 different ANN structures were considered by progressively increasing the number of hidden neurons from 1 to 20. For each structure, 500 ANN realizations, different for neural initialization, were considered; initialization was performed by randomly assigning values to both neuron weights and bias. For each ANN realization, training and validation values of the area under the receiver operating characteristic (ROC) curve (AUC_{TR} and AUC_{VA}, respectively) were used for computing a weighted AUC defined as:

$$AUC_W = 0.2 \cdot AUC_{TR} + 0.8 \cdot AUC_{VA} \quad (2)$$

where weights compensate for different sizes of training and validation sets (King & Zeng, 2003). The optimal ANN structure was selected as the one characterized by the highest mean (over the 500 realizations) AUC_W value. Eventually, the optimal ANN (OANN) for assessing the hERG potassium-channel block was identified as the realization with optimal structure and highest AUC_W.

2.5 | Statistics

Normality of $ERD_{30\%}$, $T_{S/A}$, $\Delta ERD_{30\%}$, $\Delta T_{S/A}$, B(%) and D distributions were evaluated using Lilliefors' test. Normal feature distributions were described in terms of mean ± standard deviation (SD) and compared with the paired-sample t test for equal means. Non-normal feature distributions were described in terms of 50th [25th;75th] percentiles and compared using the Wilcoxon signed rank test for equal medians (i.e., 50th percentile). Statistical significance level was set at 0.05 in all cases.

To evaluate goodness of OANN-based classification, plasma-based HB\LB classification was taken as the gold standard. The cases classified as HB by both plasma measurements and OANN were considered as true positive (TP); the cases classified as LB by both plasma measurements and OANN were considered as true negative (TN); the cases classified as HB by plasma measurements and LB by OANN were considered as false negative (FN); eventually, the cases classified as LB by plasma measurements and HB by OANN were considered as false positive (FP). Accordingly, to evaluate OANN performances, sensitivity (Se), specificity (Sp), accuracy (Ac), and precision (Pp) were computed in correspondence with the optimal operating point (i.e., the point that minimizes erroneous classifications) of the ROC curve relative to the test set as follows:

$$Se = \frac{TP}{TP + FN} \quad (3)$$

$$Sp = \frac{TN}{TN + FP} \quad (4)$$

$$Ac = \frac{TP + TN}{TP + TN + FP + FN} \quad (5)$$

$$Pp = \frac{TP}{TP + FP}. \quad (6)$$

Thus, Se measures the percentage of HB correctly classified by OANN with respect to all HB identified by plasma measures; Sp measures the percentage of LB correctly classified by OANN with respect to all LB identified by plasma measures; Ac measures the total percentage of HB and LB correctly classified by OANN; and Pp measures the percentage of HB correctly classified by OANN with respect to all OANN HB classifications.

TABLE 1 Electrocardiographic and plasma-feature trends over time (from −0.5 to 14 hr time-points)

Time-points (hr)	*D* (nmol/L)	*B*(%)	$ERD_{30\%}$ (ms)	$T_{S/A}$ (per s)
−0.5	0.00 ± 0.00	0.00 ± 0.00	43.0 [41.3;46.7]	11.29 ± 0.93
1.0	3.30 ± 1.65***	63.84 ± 11.41***	47.7 [44.7;54.7]***	10.16 ± 1.32***
1.5	4.17 ± 1.15***	69.49 ± 4.37***	55.8 [49.7;62.0]***	9.04 ± 1.22***
2.0	5.47 ± 0.79***	73.33 ± 1.80***	61.2 [57.0;72.7]***	7.93 ± 1.59***
2.5	5.96 ± 0.78***	74.34 ± 1.58***	63.0 [57.3;69.3]***	6.67 ± 2.01***
3.0	5.58 ± 0.68***	73.62 ± 1.48***	62.0 [55.3;75.3]***	7.14 ± 1.91***
3.5	4.81 ± 0.69***	71.80 ± 1.87***	61.2 [56.0;74.0]***	8.05 ± 1.51***
4.0	4.75 ± 0.71***	71.64 ± 1.89***	60.3 [53.3;63.3]***	7.94 ± 1.65***
5.0	3.86 ± 0.45***	69.13 ± 1.49***	54.2 [51.0;62.3]***	8.40 ± 1.75***
6.0	3.68 ± 0.54***	68.45 ± 2.01***	56.7 [52.3;66.7]***	8.84 ± 1.99***
7.0	3.13 ± 0.44***	66.31 ± 1.90***	53.7 [51.3;63.7]***	9.41 ± 1.53***
8.0	2.73 ± 0.34***	64.50 ± 1.70***	53.3 [47.0;58.3]***	9.61 ± 1.64***
12.0	1.62 ± 0.22***	57.00 ± 2.07***	45.3 [43.3;50.7]**	10.85 ± 1.20*
14.0	1.40 ± 0.35***	54.56 ± 3.35***	44.5 [42.0;49.3]*	11.06 ± 1.49

*$p < .05$; **$p < .01$; ***$p < .001$ when comparing postdose vs predose levels.

3 | RESULTS

Feature trends over time (from −0.5 to 14 hr time-points) are reported in Table 1 and shown in Figure 1, where individual distributions are also depicted. $ERD_{30\%}$ was the only feature characterized by a non-normal distribution. Both $ERD_{30\%}$ and $T_{S/A}$ were altered by the dofetilide administration and reached their maximum difference (with respect to their predose levels) at 2.5 hr time-point (i.e., at the time-point in which both *D* and *B*(%) were maximum) to then turn toward their basal levels. Differently from $T_{S/A}$, at 14 hr time-point, $ERD_{30\%}$ was still not completely returned to its predose level, and *D* and *B*(%) were still greater than zero.

According to *B*(%), training set contained 95 HB cases and 19 LB cases, while validation set contained 24 HB cases and 5 LB cases. Training and validation sets were used to identify OANN, which was characterized by 18 neurons in the hidden layer (Figure 2). When applied to the test set, which according to *B*(%) was composed of 119 HB cases and 24 LB cases, OANN provided a ROC with an AUC of 0.91 (Figure 3). The contingency table is reported in Table 2. Values of Se, Sp, Ac, and Pp were 0.93, 0.83, 0.92, and 0.96, respectively.

4 | DISCUSSION

This study proposed an ANN-based model for classification of the hERG potassium-channel block based on ECG features characterizing the T wave. Specifically, two features, namely $ERD_{30\%}$ and $T_{S/A,}$ were used as ANN input. ANN-based classification of the hERG block was made in terms of high- (HB) and low- (LB) block percentage, using 60% block as threshold. Eventually, OANN was identified by using ECG data recorded at different time-points from dofetilide administration (from −0.5 to 14 hr) and by comparing the ANN-based hERG block classification against classification from the plasma measurements, the latter used as the gold standard.

Pharmacokinetics as well as features trends over time have been shown not to differ considerably among subjects (Figure 1), thus confirming that ECG-based features are adequate ANN input features to discriminate high from low block. As for the input feature selection, $ERD_{30\%}$ and $T_{S/A}$ were chosen among all the features that are known to correlate with the hERG channel block, namely $T_{S/A}$, T_pT_e, $ERD_{30\%}$, and $LRD_{30\%}$ (i.e., 30% late repolarization delay) (De Bie et al., 2017; Vicente et al., 2015). Additionally, ECG features showing correlation with blood potassium concentration were also investigated, since hERG block and hypokalemia result in similar outcomes in terms of QT-interval prolongation and reduced T-wave amplitude (De Bie et al., 2017; Diercks, Shumaik, Harrigan, Brady, & Chan, 2004). The list of features correlating with blood potassium concentration included T_{RS}, T_A, T_{COG} (i.e., T-wave center of gravity) and T/R_A (i.e., the ratio between the amplitude of T and R waves), as well as $T_{S/A}$ (Corsi et al., 2017; Dillon et al., 2015). Thus, $T_{S/A}$ was chosen since it is a strong predictor of both hERG channel block and blood potassium level (De Bie et al., 2017). Being $T_{S/A}$ a reliable descriptor of the late phase of repolarization, $ERD_{30\%}$ was chosen as an independent (from multicollinearity testing) ECG feature related to the early phase of repolarization. Indeed, both the early and the late phases of repolarization are known to be affected by hERG block (Johannesen, Vicente, Mason, et al., 2014). With respect to $T_{S/A}$, which returns to pre-administration values within 12 hr, alterations in $ERD_{30\%}$ last longer and follow the persistent hERG block (as detected by plasma measurements) for at least 14 hr (Table 1). This observation suggests that dofetilide, as pure hERG blocking drug, affects more early than late phase of repolarization, thus corroborating significance of $ERD_{30\%}$, in addition to $T_{S/A}$ in the classification of hERG block.

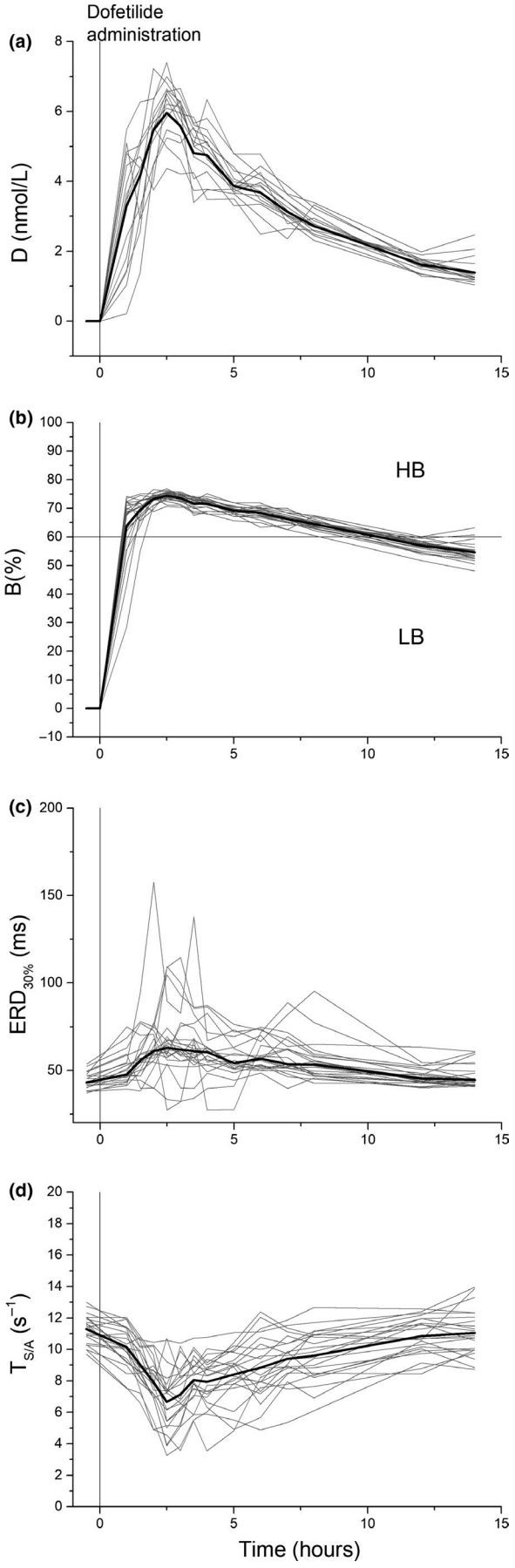

FIGURE 1 Individual (gray lines) and mean/median (black lines) distributions of the features over time; D (nmol/L), dofetilide plasma concentration (panel a); B(%), percentage of hERG potassium-channel block (panel b); $ERD_{30\%}$ (ms), 30% early phase of repolarization duration (panel c); and $T_{S/A}$ (per s), ratio of downgoing T-wave slope and T-wave amplitude (panel d)

The OANN classification of the hERG block was performed by using individual differences in T-wave morphology from their baseline values and not their absolute values. Indeed, we know from literature (Vicente et al., 2015) that changes in T-wave morphology could provide specific information to discriminate between high and low risk of torsade de pointes. Thus, we had to refer to changes with respect to baseline values ($\Delta ERD_{30\%}$ and $\Delta T_{S/A}$ values) and not to their actual values ($ERD_{30\%}$ and $T_{S/A}$).

ECG-based hERG block classification is noninvasive and thus preferable over plasma-based hERG block classification. However, being based on ECG features, it can be performed only in the time interval during which the presence of the drug causes ECG changes (particularly T-wave changes, being $ERD_{30\%}$ and $T_{S/A}$ used as input features of OANN). Such interval does not necessarily match the time interval needed by the drug to be completely washed out. In the present study, dofetilide was used, and OANN performance was evaluated in the time interval going from 1 to 14 hr after dofetilide administration (Table 1). Indeed, no important pharmacokinetic issue occurred in this time interval, being dofetilide distribution into the effect compartment already completed after 1 hr and total elimination of the drug not yet reached at 14 hr after oral administration (Lenz & Hilleman, 2000) (Table 1).

OANN was efficient in detecting high hERG block (Se = 0.93 in the test set). A little less efficient performance was provided by OANN when detecting low hERG block (Sp = 0.83 in the test set). However, this result could be due to the low number of LB cases in the dataset (overall, 48 LB cases out of 286, with only 24 cases in the test set, as by plasma-based classification, Table 2). Overall, OANN showed good HB\LB classification performances (Ac = 0.92 and Pp = 0.96 in the test set).

The results of this study demonstrate that OANN reliably assesses hERG block in the presence of pure hERG blocking drugs, such as dofetilide. Indeed, pure hERG blocking drugs affect both the early and the late phases of repolarization (Johannesen, Vicente, Mason, et al., 2014). Other drugs causing multichannel block were shown to shorten only the early phase of repolarization (Johannesen, Vicente, Mason, et al., 2014). The ability of OANN in discriminating hERG block in multichannel block condition will be investigated in future studies. However, being $ERD_{30\%}$ a descriptor of the early phase of repolarization and being $T_{S/A}$ already tested in multichannel block conditions, it is reasonable to hypothesize that the proposed OANN-based model could be a reliable tool also in this condition.

Level of hERG potassium-channel block may increment the risk of torsade de pointes (Roden, 2016). Thus, availability of methods for automatic assessment of the hERG potassium-channel block based on changes (with respect to baseline) in T-wave features may

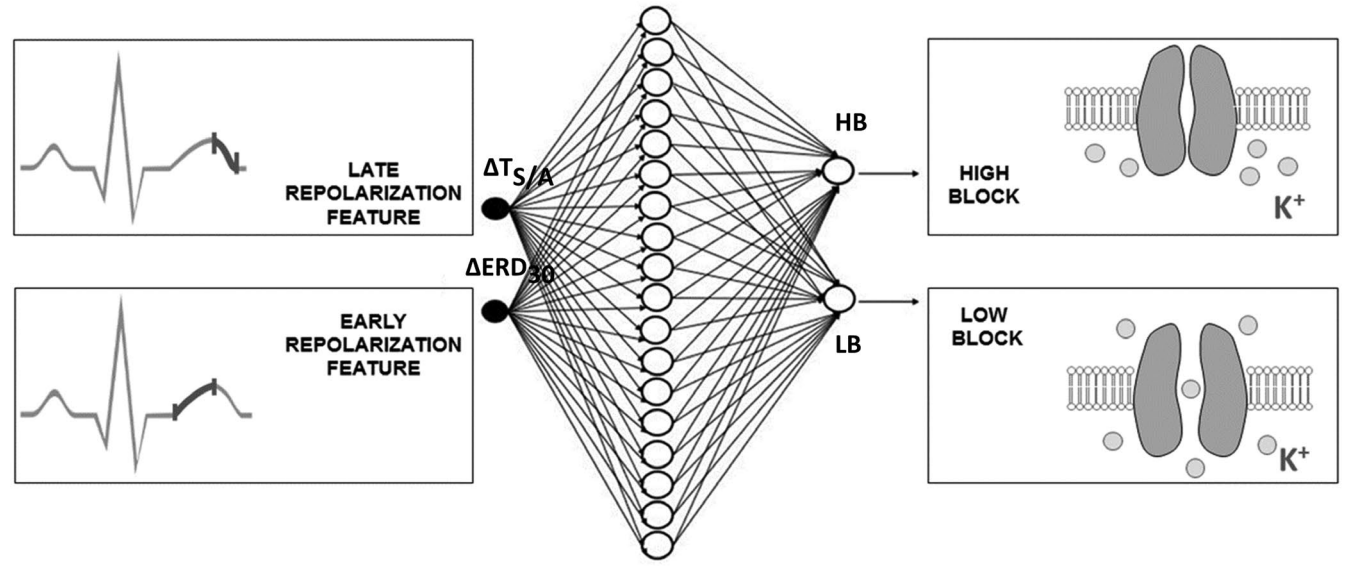

FIGURE 2 The optimal artificial neural network (OANN) for the classification of hERG block. OANN is fed by two differential electrocardiographic features ($\Delta T_{S/A}$ and $\Delta ERD_{30\%}$) and is characterized by two layers: the hidden layer, characterized by 18 neurons, and the output layer, characterized by 2 neurons for hERG block classification in two classes, high block (HB; higher than 60%) and low block (LB; not overcoming 60%)

support assessment of cardiovascular risk during some medical treatments (pharmacological or not), such as hemodialysis, in which abnormal fluctuations of the potassium concentration occur.

This study uses ANN for classification of the hERG potassium-channel block after dofetilide administration in healthy subjects. Future studies will investigate validity of this method when applied to patients, possibly with abnormal T waves. Still, we can speculate the method to work also in patients if T-wave variations are analogous to those in healthy subjects, independently from their initial T-wave morphology.

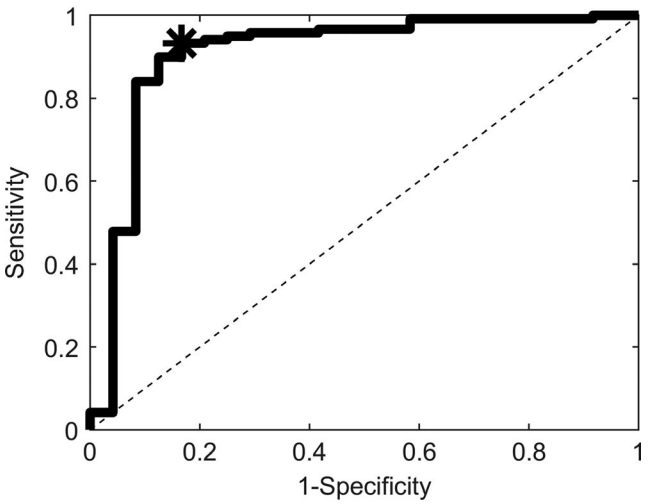

FIGURE 3 Receiver operating characteristic (ROC) obtained by applying the optimal artificial neural network (OANN) to the test set (N = 143). Area under the curve (AUC) is 0.91; Se and Sp in correspondence with the optimal point (*) are 0.93 and 0.83, respectively

In conclusion, this study proposes OANN as a reliable model for noninvasive assessment of the hERG potassium-channel block. This new model focuses on characterization of the hERG block based on T-wave changes and was able to reliably classify hERG block in two classes: HB and LB. OANN neuron weights and biases were not reported here; however, they are available for research studies by directly contacting the corresponding author (Prof. Laura Burattini, l.burattini@univpm.it).

CONFLICT OF INTEREST

All authors have no financial and personal relationships with other people or organizations that could inappropriately bias the work.

ETHICAL APPROVAL

Data used in the present study are available from Physionet. All data from Physionet have been fully de-identified and may be used without further independent ethics committee approval.

TABLE 2 Contingency table for evaluating classification in high-block (HB) and low-block (LB) classes based on the optimal artificial neural network (OANN) against that based on plasma measurements, taken as gold standard

		Plasma-based classification		
		HB	LB	TOT
OANN-based classification	HB	110	4	114
	LB	9	20	29
	TOT	119	24	143

ORCID

Laura Burattini https://orcid.org/0000-0002-9474-7046

REFERENCES

Abraham, J. M., Saliba, W. I., Vekstein, C., Lawrence, D., Bhargava, M., Bassiouny, M., … Wilkoff, B. L. (2015). Safety of oral dofetilide for rhythm control of atrial fibrillation and atrial flutter. *Circulation: Arrhythmia and Electrophysiology*, *8*, 772–776. https://doi.org/10.1161/circep.114.002339

Bishop, C. (2006). *Pattern recognition and machine learning*, 1st ed. New York, NY: Springer-Verlag.

Corsi, C., Cortesi, M., Callisesi, G., De Bie, J., Napolitano, C., Santoro, A., … Severi, S. (2017). Noninvasive quantification of blood potassium concentration from ECG in hemodialysis patients. *Scientific Reports*, *7*, 42492. https://doi.org/10.1038/srep42492

Crumb, W. J., Vicente, J., Johannesen, L., & Strauss, D. G. (2016). An evaluation of 30 clinical drugs against the comprehensive in vitro proarrhythmia assay (CiPA) proposed ion channel panel. *Journal of Pharmacological and Toxicological Methods*, *81*, 251–262. https://doi.org/10.1016/j.vascn.2016.03.009

De Bie, J., Chiu, B., Mortara, D., Corsi, C., & Severi, S. (2017). Quantification of hERG Block from the ECG. *Computing in Cardiology*, *44*, 1–4. https://doi.org/10.22489/CinC.2017.239-123

Diercks, D. B., Shumaik, G. M., Harrigan, R. A., Brady, W. J., & Chan, T. C. (2004). Electrocardiographic manifestations: Electrolyte abnormalities. *Journal of Emergency Medicine*, *27*, 153–160. https://doi.org/10.1016/j.jemermed.2004.04.006

Dillon, J. J., Desimone, C. V., Sapir, Y., Somers, V. K., Dugan, J. L., Bruce, C. J., … Friedman, P. A. (2015). Noninvasive potassium determination using a mathematically processed ECG: Proof of concept for a novel "blood-less, blood test". *Journal of Electrocardiology*, *48*, 12–18. https://doi.org/10.1016/j.jelectrocard.2014.10.002

Goldberger, A. L., Amaral, L. A. N., Glass, L., Hausdorff, J. M., Ivanov, P. C., Mark, R. G., … Stanley, H. E. (2000). PhysioBank, PhysioToolkit, and PhysioNet: Components of a new research resource for complex physiologic signals. *Circulation*, *101*, e215–e220. https://doi.org/10.1161/01.CIR.101.23.e215

Hagan, M. T., & Menhaj, M. B. (1994). Training feedforward networks with the Marquardt algorithm. *IEEE Transactions on Neural Networks*, *5*, 989–993. https://doi.org/10.1109/72.329697

Johannesen, L., Vicente, J., Gray, R. A., Galeotti, L., Loring, Z., Garnett, C. E., … Strauss, D. G. (2014). Improving the assessment of heart toxicity for all new drugs through translational regulatory science. *Clinical Pharmacology and Therapeutics*, *95*, 501–508. https://doi.org/10.1038/clpt.2013.238

Johannesen, L., Vicente, J., Mason, J. W., Sanabria, C., Waite-Labott, K., Hong, M., … Strauss, S. G. (2014). Differentiating drug-induced multichannel block on the electrocardiogram: Randomized study of dofetilide, quinidine, ranolazine, and verapamil. *Clinical Pharmacology and Therapeutics*, *96*, 549–558. https://doi.org/10.1038/clpt.2014.155

King, G., & Zeng, L. (2003). Logistic regression in rare events data. *Journal of Statistical Software*, *8*, 137–163.

Lenz, T. L., & Hilleman, D. E. (2000). Dofetilide, a new class III antiarrhythmic agent. *Pharmacotherapy*, *20*, 776–786. https://doi.org/10.1592/phco.20.9.776.35208

Mitcheson, J. S., Chen, J., Lin, M., Culberson, C., & Sanguinetti, M. C. (2000). A structural basis for drug-induced long QT syndrome. *Proceedings of the National Academy of Sciences of the United States of America*, *97*, 12329–12333. https://doi.org/10.1073/pnas.210244497

Roden, D. M. (2016). Predicting drug-induced QT prolongation and torsades de pointes. *Journal of Physiology*, *594*, 2459–2468. https://doi.org/10.1113/JP270526

Vicente, J., Johannesen, L., Mason, J. W., Crumb, W. J., Pueyo, E., Stockbridge, N., & Strauss, D. G. (2015). Comprehensive T wave morphology assessment in a randomized clinical study of dofetilide, quinidine, ranolazine, and verapamil. *Journal of the American Heart Association*, *4*, 1–13. https://doi.org/10.1161/JAHA.114.001615

How to cite this article: Morettini M, Peroni C, Sbrollini A, Marcantoni I, Burattini L. Classification of drug-induced hERG potassium-channel block from electrocardiographic T-wave features using artificial neural networks. *Ann Noninvasive Electrocardiol*. 2019;24:e12679. https://doi.org/10.1111/anec.12679